Turbulence intensity within large offshore wind farms

PLEASE CITE THE PUBLISHED VERSION

http://www.ewea.org/annual2015/wp-content/uploads/files/conference/scientific-proceedings/2015-EWEA-scientific-proceedings.pdf

PUBLISHER

European Wind Energy Association

VERSION

VoR (Version of Record)

PUBLISHER STATEMENT

LICENCE

REPOSITORY RECORD

TURBULENCE INTENSITY WITHIN LARGE OFFSHORE WIND FARMS

Peter Argyle[1], Simon Watson[1], Christiane Montavon[2], Ian Jones[2], Megan Smith[3]
[1] CREST, Holywell Park, Loughborough University, Loughborough, UK
[2] ANSYS UK Ltd, 97 Jubilee Avenue, Milton Park, Abingdon, UK.
[3] The Carbon Trust, 27-45 Stamford Street, London, UK.
p.argyle@lboro.ac.uk, s.j.watson@lboro.ac.uk, christiane.montavon@ansys.com, ian.jones@ansys.com,
megan.smith@carbontrust.com

ABSTRACT: The so-called Frandsen model forms the basis for the assessment of wind farm level turbulence intensity (TI) in the IEC standard 61400-1 edition 3. It is used in the choice of turbine suitable for a particular wind farm site. The Frandsen model was developed several years ago using field data when turbines and wind farms were of smaller scale than today. There is now an interest in the accuracy of models such as that of Frandsen when applied to the scale of the largest offshore wind farms. In this paper, we present the results of an analysis of the accuracy of the Frandsen model in predicting TI within the Greater Gabbard offshore wind farm. A comparison is made between measured data and predictions from: 1) the original Frandsen model; 2) a simplified version of the Frandsen model and 3) output from the ANSYS WindModeller CFD model. In general, the Frandsen model was found to perform well in the prediction of mean levels of TI but less well than a simplified model using either a freestream ambient TI or a turbine wake TI regardless of distance. Representative or 90% percentile TI levels are less well predicted under direct wake conditions due to the lack of consideration of turbine generated variance in turbulence and the manner in which the 90% percentile freestream TI is incorporated. ANSYS WindModeller was found to perform well in the prediction of mean TI and has the benefit of not requiring upstream TI data. The CFD model can be used to predict representative TI, when complemented with a model for the variance of turbulence. Predictions from the Frandsen model are more sensitive to the choice of freestream data than those from the CFD model.

1. INTRODUCTION

The fluctuations of the wind speed caused by turbulence affect the fatigue of the turbine blades and tower and consequently the turbine lifetime. As shown in Frandsen [1], wind turbine loads, for a given wind speed, are mostly conditioned by the level of turbulence intensity (TI) in the flow, and more specifically by the longitudinal component σ_u of the velocity fluctuation along the main flow direction. For turbines within a large array, operating in wake conditions, the Frandsen model [1] for TI is used as the basis for the IEC Standard 61400-1 edition 3, amendment 1 [2] to derive an effective TI as a function of wind speed. Turbine suitability is assessed by verifying that the site effective TI is below the turbine design TI for the range of wind speed between 60% of the rated wind speed and the cut-out wind speed.

This paper summarises work carried out as part of the Carbon Trust's Offshore Wind Accelerator's project `*Validation of Frandsen Turbulence Intensity Model and Large Wind Farm Models*` [3]. The objective of this work is to assess the performance of 1) the Frandsen model and 2) a computational fluid dynamics (CFD) code in predicting levels of turbulence intensity within a large wind farm by comparing data from the Greater Gabbard wind farm with model predictions.

2. SITE

The wind farm investigated is that of Greater Gabbard, situated in the North Sea, with a layout as shown in Figure 1. It consists of two sections, one to the North with 102 Siemens 3.6MW turbines ($h_{hub} = 77.5$ m , $D = 107$ m) and one to the South, with 38 turbines. The distance between the southern and northern part of the array is over 70D. For the flow directions with regular spacing, turbines are separated by typically ~9.7D (200˚), ~10D (247˚) and ~8.3D (315˚). The site has two meteorological masts, marked by squares in Figure 1: IGMMX to the south of the Northerly section, 2.5D upstream of a turbine, and IGMMZ embedded within the Northerly section. SCADA data from each turbine alongside measurements collected at the two masts were made available for the project by the operator SSE. Two turbines, IGH08 and IGK02, are marked as black circles in Figure 1 and were used to validate model predictions in addition to the two met masts.

To provide a representation of the freestream wind conditions, a data set was constructed from a selection of upstream turbines with the

freestream wind direction calculated by averaging the yaw position of the six turbines highlighted as open circles in Figure 1, whilst the freestream wind speed values were calculated by averaging the SCADA measurements from these turbines when they were individually considered by direction to be in the freestream flow. Note that the local wind speed for the turbines is derived from nacelle anemometry. The accuracy of using nacelle wind speed to derive turbine upstream conditions was assessed, by correlating the wind speed measured at IGMMX with that measured at IGF10 (2.5D downstream of the mast). For the wind speed, the linear correlation between mast and turbine was good albeit that the slope of the regression line is not exactly 1 (Figure 2). For the wind speed standard deviation, the correlation is less good, and the ratio $\sigma_{IGF10}/\sigma_{mast}$ shows values below 1 at low wind speeds (Figure 3). There are some important caveats to the use of either turbine data or mast data for inferring the freestream wind speed and TI in this study:

- Nacelle anemometers are in the wake of the rotor and their measurements are normally corrected to provide 'freestream' values. This process introduces a degree of uncertainty and is known to lack rigour when trying to measure true freestream wind speed;
- Nacelle anemometers will measure additional turbulent components that result from the blades as well as structures on the nacelle, e.g. hand-rails;
- The limited numbers of pulses per revolution from the anemometers on IGMMX meant that the recording of turbulent fluctuations at low wind speed values (especially below 8m/s) was subject to error.

These factors are discussed later when validating model predictions.

For the comparisons between model and data for the TI by direction in section 4.1, the data were binned by freestream wind speed, and results are shown for the 10m/s (±0.5m/s) bin. The corresponding wind rose at 10 m/s is shown in Figure 4.
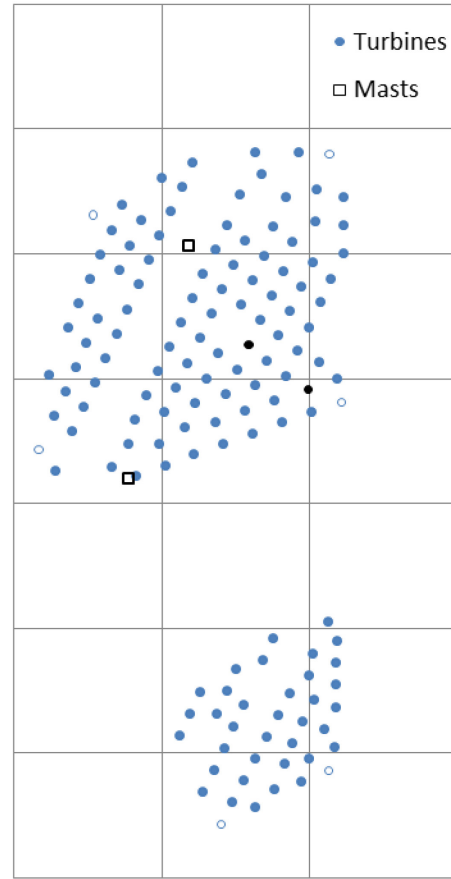

Figure 1: Layout of Greater Gabbard Wind Farm. Turbines marked in black are IGH08 (top left) and IGK02 (bottom right), the met masts are shown as squares and the six turbines used to calculate freestream conditions are shown as open circles.
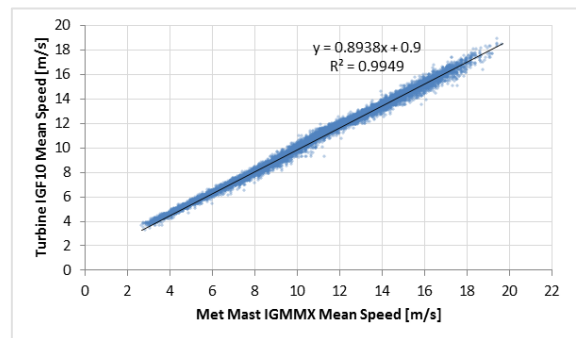

Figure 2: Correlation between wind speed at IGF10 and mast IGMMX, for directions 180°<θ<250° where neither are influenced by upstream turbines.

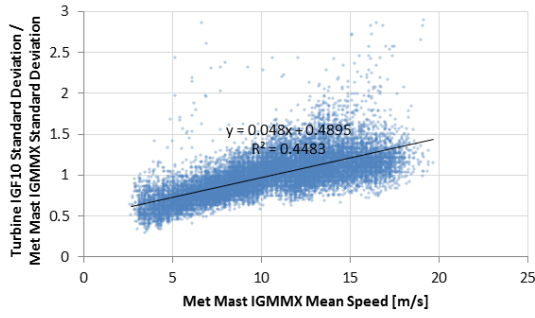Figure 3: Ratio between wind speed standard deviation at IGF10 and IGMMX against mast wind speed, for directions 180°<θ<250° where neither are influenced by upstream turbines.
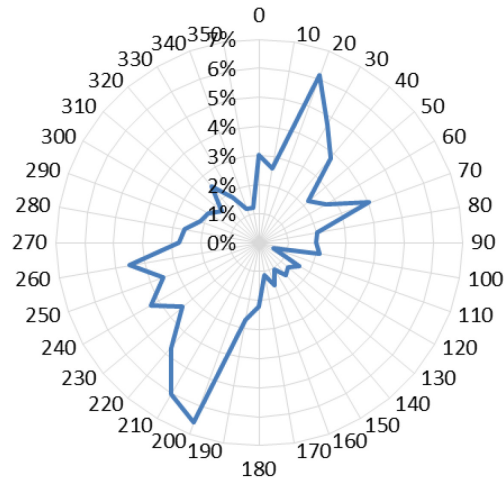

Figure 4. Freestream wind rose for 10m/s wind speed.

With potential problems associated with using nacelle anemometry, a second data set to represent the wind farm upstream conditions was generated by comparing the measurements from mast IGMMX and the wind turbine IGF10 located just 2.5 diameters away. Assuming the systematic bias in mean wind speed measurements between IGMMX and IGF10 is a constant feature of using data from turbine nacelles, the values of nacelle-measured mean wind speed were adjusted to the corresponding values of a mast-measured data set.

3. TURBULENCE INTENSITY

3.1 Frandsen model

The Frandsen model for the effective TI ($I_{eff}(U)$) is providing a local TI at a location within the wind farm, but is specified in terms of wind farm upstream conditions (i.e. conditions which can be measured before the wind farm is operational). It is summarised below, using the representative (i.e. the 90th centile value of the) wind speed standard deviation in the integrand.

$$I_{eff}(U) = \left[\int_{-180}^{180} I^m f_{wd}(\theta|U_0)d\theta \right]^{\frac{1}{m}}$$
$$I = \frac{\sigma(\theta,U)}{U} \tag{1}$$

where m is the Wöhler exponent, θ is the wind direction, and U is the wind speed. The value of $\sigma(\theta,U)$ is calculated depending on location within the wind farm with respect to wind direction and assuming a regular turbine layout, via one of the following three equations:

$$\sigma_{repr,0} = \langle \sigma_0 \rangle + 1.28 stdev(\sigma_0) \tag{2}$$

$$\sigma_{repr,0,wf} = \langle \sigma_{0,wf} \rangle + 1.28 stdev(\sigma_0) \tag{3}$$

$$\sigma_{0,wake} = \sqrt{\frac{U_0^2}{\left(1.5 + 0.8\frac{d_i}{\sqrt{C_T}}\right)^2} + \sigma_{repr,0}^2} \tag{4}$$

where $\sigma_{repr,0}$ is the representative wind speed standard deviation of the freestream flow, $\sigma_{repr,0,wf}$ is the representative wind speed standard deviation of the flow within an infinite array, $\sigma_{0,wake}$ is the representative wind speed standard deviation of the flow directly within the wake of an upstream turbine, d_i is the normalised distance to the upstream turbine, C_T is the turbine thrust coefficient. Chevron brackets indicate ensemble averaging. The wind farm ambient (or background) wind speed standard deviation, $\sigma_{0,wf}$, is calculated from the freestream ambient background (σ_0) and wind farm added wind speed standard deviation above the wind farm, $\sigma_{add,wf}$, as follows:

$$\sigma_{0,wf} = \frac{1}{2}\left(\sqrt{\sigma_{add,wf}^2 + \sigma_0^2} + \sigma_0 \right) \tag{5}$$

$$\sigma_{add,wf} = \frac{0.36U_0}{1 + 0.2\sqrt{s_f s_r/C_T}} \tag{6}$$

where s_f and s_r are the normalised distances between turbines in a row and between turbine rows respectively. The Frandsen model stipulates that equation (4) shall be used, if the location is in the direct wake of a turbine less than 10 rotor diameters away. For directions with turbines more than 10 diameters away, where there are more than 5 turbines between

the selected location and the edge of the wind farm or if the turbine separation is less than 3 diameters, Equation (3) shall be used. For all other directions (no turbine or less than 5 turbines upstream, all of them beyond 10D), the ambient TI calculated via Equation (2) is valid. Frandsen fitted his model for the direct wake contribution using data from the Vindeby, Andros, Taff Ely and Alsvik wind farms [1] and therefore there may be aspects of the model which are not suitable for modern offshore farms that are much larger. An example of this is the arbitrary 10 diameter cut-off applied to determine whether an individual turbine wake is significant to the TI measured at any particular location. To test the applicability of the 10 diameter cut-off, this work will also investigate a `Simplified` version of the model which does not utilise the infinite array concept. Thus, for the Simplified model, if a turbine exists upstream of a specified location for the wind direction of interest, Equation (4) shall be used, irrespective of its distance, whilst Equation (2) shall be used for all other directions at that location.

3.2 CFD simulations

CFD simulations were carried out using ANSYS WindModeller modelling the wakes with an actuator disk method under neutral atmospheric conditions. Turbulence closure is provided using a k-ε model with modified turbulence constants (C_μ = 0.03, turbulence decay rate = 0.6), as successfully validated in earlier work [6]. For the results shown here, only the Northern section was modelled, using a simulation domain with a 17km radius, and 5 km height. Separate simulations for the entire wind farm showed that the effect of the Southern section is only minimal (increasing the TI from 5.8% to 7.1% for mast IGMMX) and only affected the sectors 130˚ to 170˚. The mesh resolution used a background horizontal resolution of 60m. In the vertical, the mesh resolution follows a geometric progression, with a first cell height of 2m, and an expansion factor of 1.16. Simulations have been carried out for 36 equally spaced directions, and 4 reference wind speeds (6, 10, 12 and 14 m/s) at hub height.

When carrying out Reynolds Averaged Navier-Stokes (RANS) simulations, solving for stationary flow conditions, the resulting flow fields are assumed to be representing the mean flow conditions on site. The mean turbulence intensity from the CFD is calculated from:

$$I_{mean} = \frac{\sigma_u}{U} = \frac{\sqrt{\frac{2}{3}k}}{U} \tag{7}$$

When calculating the local TI at mast locations from the model, local values for the turbulence kinetic energy k and the wind speed U are used. For turbine locations, equation (7) is evaluated using the local value for the turbulence kinetic energy k and the turbine upstream wind speed $U_{WT,upstr}$, itself derived from the local wind speed at hub height, using 1D actuator disk theory. The reason for using the turbine upstream wind speed, is an attempt to mimic what is reported in the wind turbine SCADA data, where, via the use of nacelle transfer functions, the turbine wind speed is supposed to be representative of the wind speed upstream of the turbine.

4. COMPARISON WITH DATA

4.1 TI by direction

The results of applying the Frandsen model and the Simplified model are shown for the two met masts in Figure 5 and Figure 6 compared to values of TI measured on each mast, with freestream values indicated. The resulting mean TI from the CFD model is also shown.
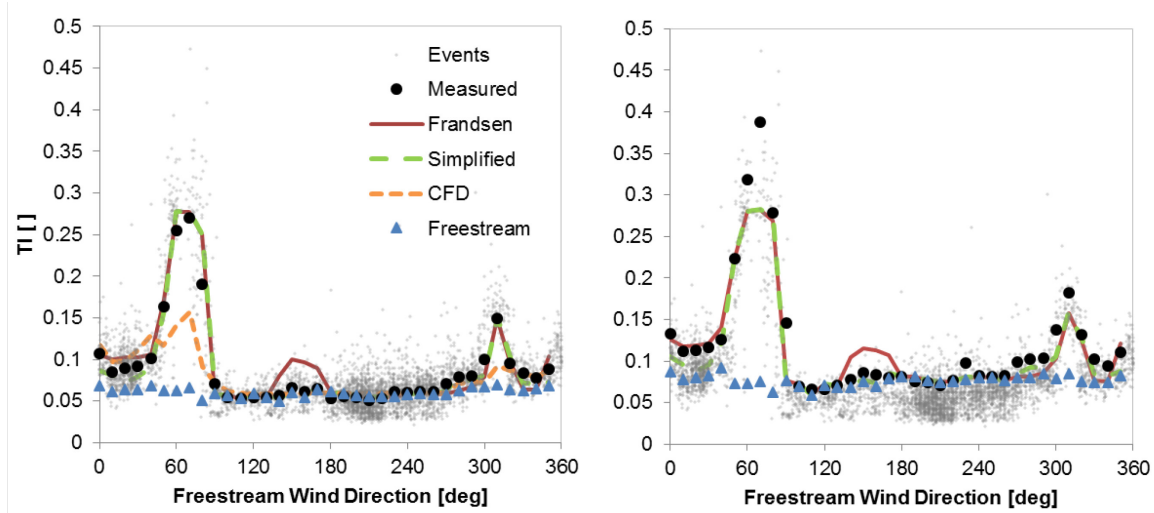
Figure 5: Mean (left) and representative (right) values of TI for the southern met mast IGMMX for a 10 m/s wind farm upstream wind speed.
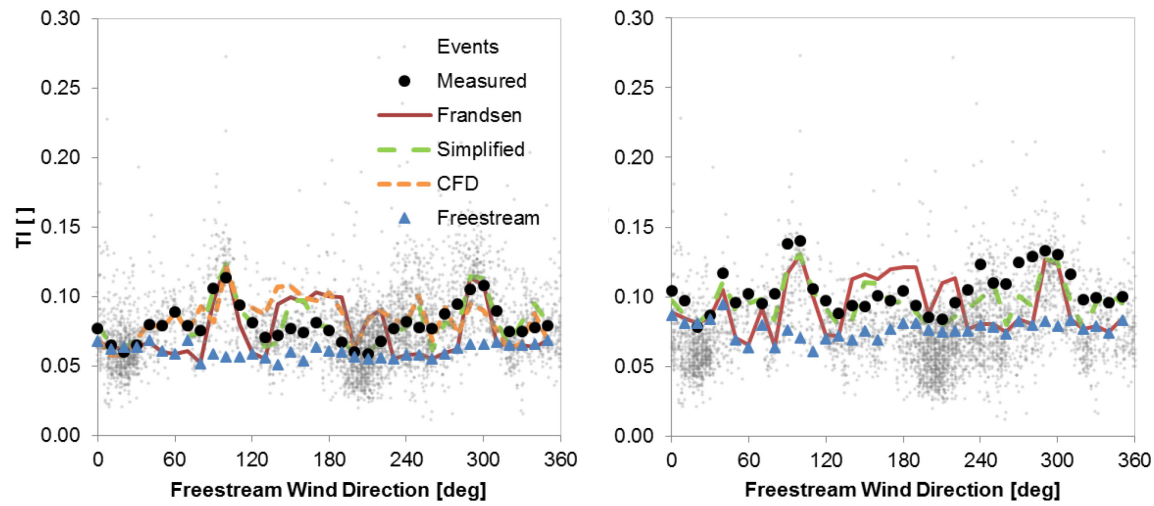

Figure 6: Mean (left) and representative (right) values of TI for the northern met mast IGMMZ.

At mast IGMMX (Figure 5) at the edge of the northern wind farm cluster, the Frandsen model provides a good prediction of the mean turbulence intensity except for the sector 0°-30° and around 150°. Between 0°-30°, the wind farm ambient TI assumed by Frandsen would seem to be an over-estimate. The over-prediction of the TI around sector 150° would seem to result from the wind farm ambient TI associated with the Southern section. Arguably, the wind farm ambient TI in the Frandsen model is not intended to cater for the effect of a separate section of the wind farm so far upstream. The Simplified model seems to predict much better the TI in these sectors.

The CFD model provides a reasonably good prediction of the background TI, which affects the majority of directions at mast IGMMX, but tends to underestimate the peak TI in the direct wake (sector 60° and 310°). Additional simulations at a finer horizontal resolution showed that the peak TI in the near wake is not mesh converged. Further refining the mesh allows the capture of the peak in the near wake more accurately (not shown).

For directions in the direct wake of a turbine less than 10D upstream (sectors 60° and 310°), the difference between the mean and representative TI from the Frandsen and Simplified models is small. This may be because the calculation of the representative values in the wake only accounts for fluctuation of the standard deviation in the background flow and not the direct wake. The fact that the model underestimates the representative TI around these sectors may be an indication that the representative TI in the direct wake should be derived in a more sophisticated way. In particular, the inclusion of the standard deviation of the wind speed standard deviation under the square root in equation (4) is questionable. Doing so means that, for a given

value of background fluctuation $stdev(\sigma_0)$, the absolute change between σ_{repr} and σ_{mean} in wake conditions, which should be a measure of $1.28\,stdev(\sigma)$ in wake conditions, is smaller than the $1.28\,stdev(\sigma_0)$ that results in freestream conditions. This is in contrast to what we see in the data at IGMMX for example, where $stdev(\sigma)$ for waked sectors tends to be larger than for freestream sectors. It is suggested that the representative σ might be better captured with:

$$\sigma_{0,wake} = \sqrt{\dfrac{U_0^2}{\left(1.5 + 0.8\dfrac{d_i}{\sqrt{C_T}}\right)^2} + \sigma_0^2}$$

$$+1.28stdev(\sigma_0\ )\qquad(8)$$

Figure 6 suggests that deep within the wind farm the Simplified model predicts the mean TI well, except near the sector 260˚ and 330˚. The overestimation around the sector 150˚ was found to be due to reduced availability of turbine IGE06, 11.3D upstream of the mast. The Frandsen model struggles in capturing trends in mean TI with direction at mast IGMMZ, sometimes underestimating where less than five turbines upstream are present, or

over-estimating for directions where the wind farm ambient TI over-predicts the actual TI.

The CFD results show a similar trend to the Simplified model, with reasonable agreement with the data, except for an underestimate of the peak around 300˚. Around sector 150˚, the CFD also produces a peak not seen in the data because of the reduced availability of turbine IGE06. Both the Frandsen and Simplified models struggle to capture the amplitude of the standard deviation of the wind speed standard deviation, underestimating the representative TI most likely for the reasons mentioned above.

Figure 7 compares the model outputs against the measured values of TI at the locations of wind turbine IGH08. In general, the Frandsen model captures the fluctuations in TI due to nearby turbines though it struggles for directions where the nearest turbine is more than 10 diameters away. For example, between 270°<θ<300°, due to the farm layout irregularity, the Frandsen model reverts to using the freestream TI value whilst between 40°<θ<120° there are less than the arbitrary 5 turbines required to suggest a wind farm TI has developed. By contrast, the Simplified model which uses the direct wake method in Equation (4) for these sectors, predicts the measured values well.
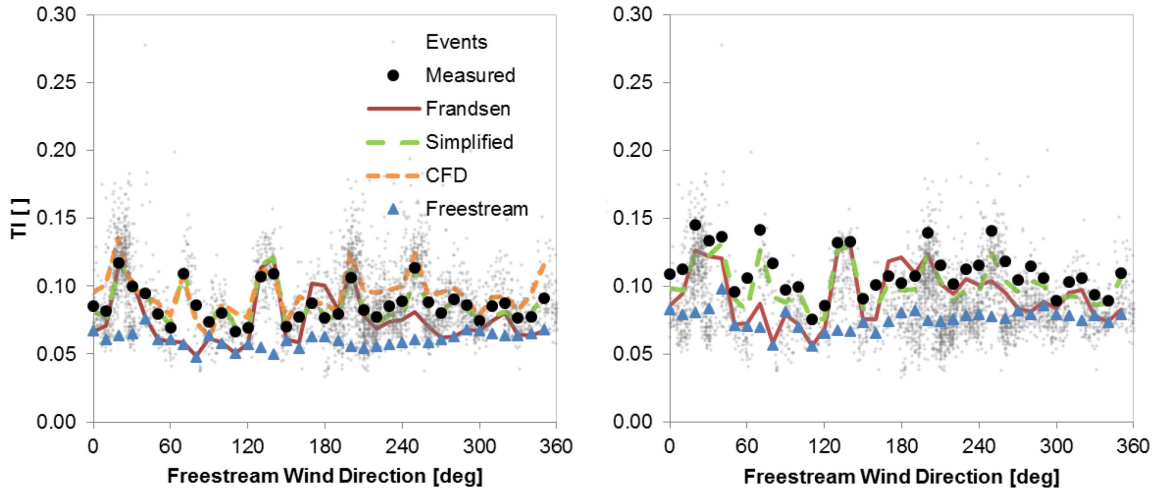

Figure 7: Mean (left) and representative (right) values of TI for the wind turbine IGH08.
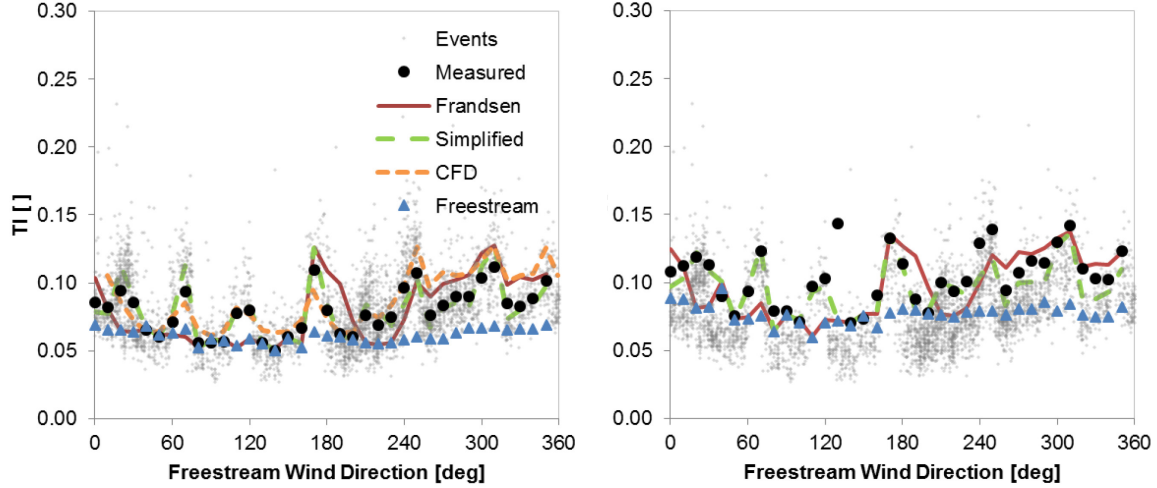
Figure 8: Mean (left) and representative (right) values of TI for the wind turbine IGK02.

Figure 8 shows results from the position of turbine IGK02 and shows similar results to Figure 7, although the proximity of the farm edge is more relevant. This is shown best for directions between 30°<θ<170° where for some directions within this sector, turbine IGK02 experiences the freestream TI values, and there are some directions which are affected by the wakes of other single turbines located further than 10 diameters. For the direction sectors relating to these distant individual turbines, the Frandsen model fails to capture the significant increases in TI whilst the results from the Simplified model agree well with the measured values.

4.2 TI vs wind speed

As would be the case for a turbine suitability assessment, we calculated the effective TI for a range of wind speed between 60% of the rated wind speed and the cut-out wind speed, evaluating equation (1) (using a Wöhler exponent m =1). As data input for this process, when using the Frandsen model, we require a data set representing the wind farm upstream conditions, characterising the ambient TI as well as the frequency distribution at each wind speed. When using a freestream data set derived from the data at mast IGMMX, we obtain the resulting $I_{eff}(U)$ curves at mast IGMMZ, which are shown in Figure 9. The results from the Frandsen and Simplified models are compared to the $I_{eff}(U)$ from the wind data and CFD results, calculated from the local TI and binned by the local wind speed at IGMMZ. When calculating the mean local TI from the CFD results shown in Figure 9, we evaluate TI directly from the solved turbulence kinetic energy, via equation (7). When using this method, the only required wind farm upstream data is the direction distribution at

any given reference wind speed. Since the CFD results are stationary solutions, for any given upstream wind speed and direction, they provide a unique value for the wind speed standard deviation, without an associated fluctuation. To derive representative TI values from the CFD, we need to complement it with a model for $stdev(\sigma)$. In the results presented in Figure 9, we used a linear relationship

$$stdev(\sigma) = aU + b$$
$$a = 0.0106, b = 0.0869 \qquad (9)$$

which was derived from correlating $stdev(\sigma)$ with U at mast IGMMX for directions unaffected by wakes. This relationship was also used when evaluating representative I_{eff} using the Frandsen and Simplified models in Figure 9, when working with upstream data derived from mast IGMMX.

When predicting the mean I_{eff}, both the Frandsen and Simplified models provide a very good prediction, between 7 and 25 m/s. Both models are reasonably close to each other, with the Frandsen model producing slightly reduced TI below 13 m/s and slightly increased TI above 13 m/s (compared to the Simplified model). At low wind speeds, the models lead to excessive effective TI values. At this point it is not clear if this is associated with potential measurement problems at mast IGMMZ, as the latter has not been maintained as thoroughly as IGMMX, and anemometers may be suffering from increased bearing friction at low wind speed (P. Housley, private communication). As described above, we also know from our data analysis that wind speed measurements from mast IGMMX seem to be affected by problems when sampling a pulsed anemometer, which leads to artificially increased wind speed standard deviations at low wind speeds. The

CFD model also performs very well between the range of wind speeds which were simulated (6-14 m/s). Outside of the simulated range, the CFD model results are not reliable as they depend on an extrapolation of the results which is not physically based.

When calculating the representative I_{eff}, both the Frandsen and Simplified models provide a good match to the measured TI between 7 and 13 m/s. At higher wind speed, these models tend to over-predict the representative I_{eff}. While we noticed from the plots by direction at 10 m/s (Figure 6) that these models tended to under-estimate the peak representative TI in wake situations, it appears that when integrating over the direction, under- and over-estimated predictions cancel out. It should be stressed that this may not be true for all wind farms or indeed for other locations in this wind farm, being dependent on the relative weighting between wake affected, wind farm affected and freestream sectors. The CFD model using the direct method and the linear expression (9) for $stdev(\sigma)$ provides an accurate effective TI for the range of simulated wind speeds.

The sensitivity of the I_{eff} predictions to the assumed wind farm upstream conditions, and in particular to the ambient $I_{eff,0}(U)$ curve, is demonstrated in Figure 10, where the I_{eff} calculations were repeated starting from a wind farm upstream data set derived from nacelle anemometry. As can be seen from these results, the effective TI derived from the Frandsen and Simplified models are very different from those obtained earlier. The predicted mean I_{eff} from these models no longer agree so well with the measured data at IGMMZ. The results from the CFD model using the direct method are unchanged. When deriving I_{eff} from a calibrated CFD model approach, the CFD model results become strongly sensitive to the ambient effective TI too.

In the calibrated approach, the wind farm upstream wind speed standard deviation is transposed to the prediction site by scaling it with the ratio of simulated standard deviation at the prediction site and upstream of the wind farm. The $I_{eff}(U)$ curves derived from the Frandsen and Simplified model, as well as from the CFD model using the calibrated approach, are very sensitive to the assumed ambient effective TI. Their overall trend is strongly reminiscent of the trend seen in the ambient conditions (plotted in Figure 11 for reference).
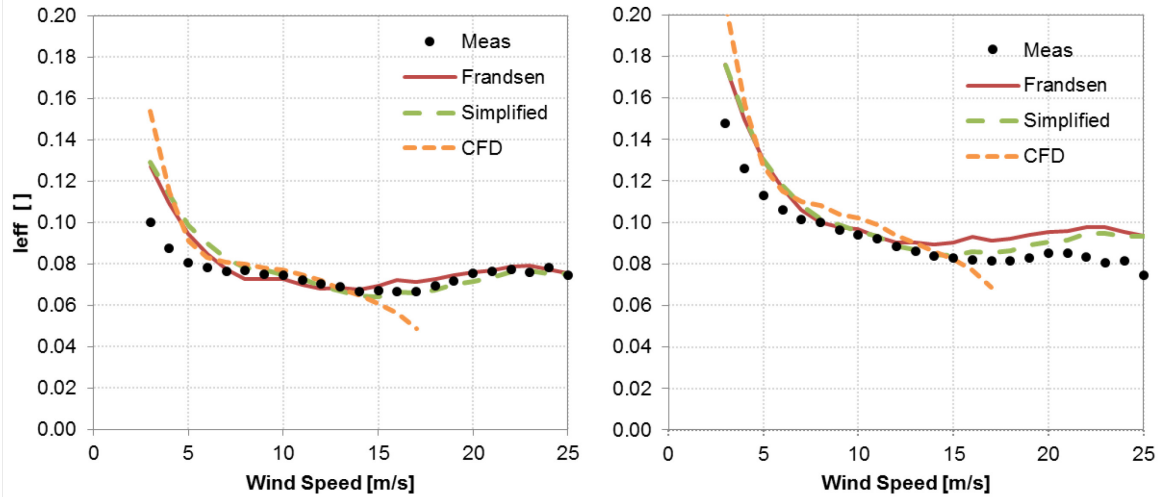

Figure 9: Mean (left) and representative (right) values of TI integrated across all directions, as measured at met mast IGMMZ, *m*=1. TI calculated using wind farm upstream conditions derived from met mast IGMMX.
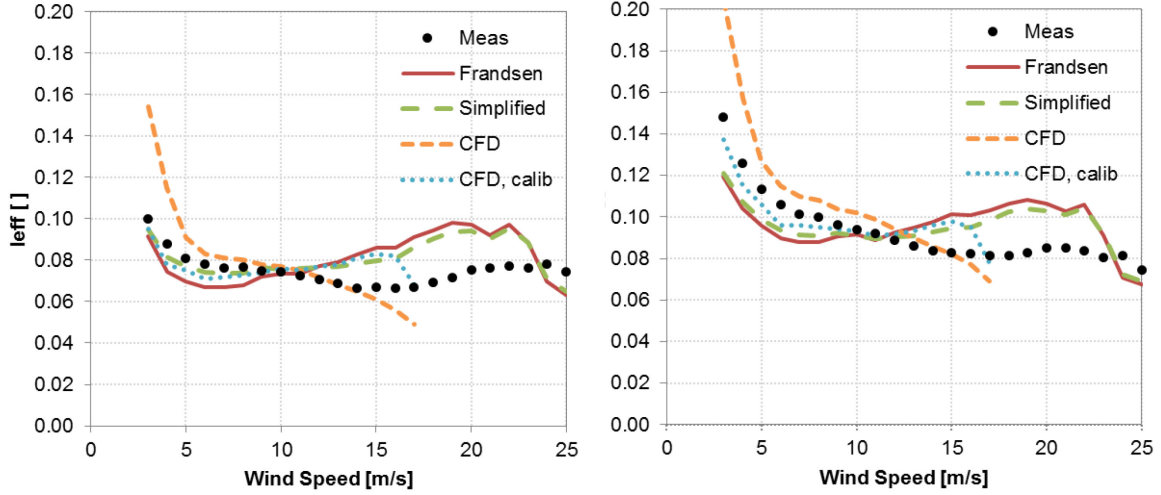
Figure 10: As Figure 9 but using wind farm upstream conditions derived from nacelle anemometry.
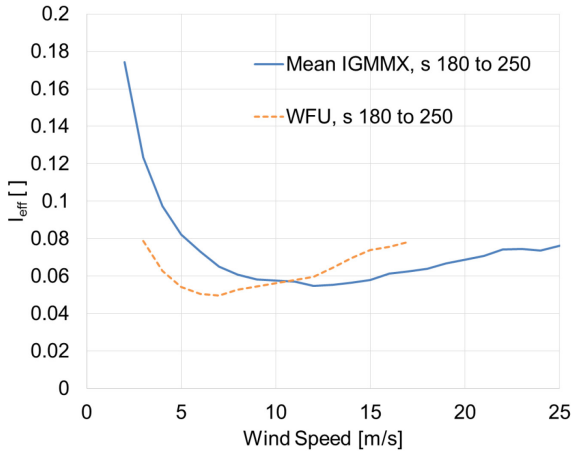

Figure 11. Ambient effective TI vs wind speed for the wind farm upstream (WFU) data set derived from data at IGMMX (continuous curve) and that derived from nacelle anemometry (dashed curve).

5. CONCLUSIONS

From the validation comparing TI vs direction at a constant wind speed of 10 m/s, we conclude that the model proposed by Frandsen for the direct wake turbulence (equation (4)) does a very good job at capturing the mean TI in the wake of a turbine, even at short range such as the 2.5D shortest distance we investigated. The use of a 10D cut-off distance beyond which the direct wake turbulence is not applied is arbitrary, and leads to significant TI peaks being missed when calculating the mean TI vs direction. Using ambient TI for directions where less than 5 turbines are located upstream beyond the 10D cut-off is also questionable as it leads to underestimated TI. Also, when applied, the wind farm background TI, tends to overestimate the measured TI. Because of all

of these observations, the Simplified model appears to provide a better agreement to the mean measured values which casts doubt on the use of a wind farm level ambient turbulence intensity.

The change in values between the mean and representative TI seen in the data set is not captured by the Frandsen model when considered by direction, likely because the model only accounts for variability in the wind speed standard deviation as present in the background flow, and no variability associated with the wakes. When averaged over all directions, the Frandsen model does a much better job in predicting this change for the case we have considered, though this is due to underestimation in some sectors and overestimation in others. This may well be wind farm and location specific and we cannot generally assume that the cancellation of errors will always lead to accurate predictions when calculating the directionally averaged value of the representative TI.

The CFD model used here is capable of capturing the key features of mean TI vs direction at the wind speed investigated, although with a tendency to under-estimate the peak TI at short range (2.5D). The derivation of an effective TI from CFD, using the direct method, also showed encouraging results for the range of wind speed simulated (6 to 14 m/s). The stationary CFD model was extended to predict representative TI by assuming a linear correlation between $stdev(\sigma)$ and the wind speed U. While this delivered good results for the site of Greater Gabbard, the applicability of the selected correlation coefficients to other sites needs to be proven.

Effective TI, when derived from the Frandsen or simplified model, as well as from the calibrated CFD model is very sensitive to the assumed

freestream conditions and results can change significantly with variations in input data. With these models, to get an accurate prediction of $I_{eff}(U)$ within the wind farm, not only is an accurate wake model required, but an accurate representation of the wind farm upstream conditions will be essential too. The CFD model using the direct method to derive TI has the advantage that it has no sensitivity to the assumed mean upstream standard deviation, instead it relies on the accuracy of the turbulence model itself.

ACKNOWLEDGEMENTS

REFERENCES

[1] S. Frandsen, "Turbulence and Turbulence Generated Loading in Wind Turbine Clusters," Risø report R-1188, 2007.

[2] IEC Standard, 61400-1, Edition 3 + Amendment 1, 2010. Wind turbines, Part 1: design Requirements, BS EN 61400-1:2005 + A1:2010.

[3] "Invitation to Tender: 'Validation of Frandsen Turbulence Intensity Model and Large Wind Farm Models' OWA Programme," [Online]. Available: http://www.carbontrust.com/about-us/work-with-us.

[4] C. Montavon, I. Jones, C. Staples, C. Strachan, I. Gutierrez, 2009, Practical issues in the use of CFD for modelling wind farms, EWEC Proceedings, Marseille.

[5] ANSYS CFX – Solver Theory Guide, Release 16.2, July 2015, ANSYS Inc.

[6] C. Montavon, I. Jones, 2013, 'Atmospheric stability and Coriolis effects in the simulation of large array losses', EWEA 2013 conference proceedings, Vienna.